

Supplementary Material to 'Global Azimuthal Anisotropy in the Transition Zone' by J. Trampert and H. J. van Heijst.

Selection of anisotropic parameters and seismic data

It is important to determine which anisotropic parameters are mapped in the most robust way from given seismic data. Two independent constraints of the so-called Love-Rayleigh incompatibility have to resolve the 5 Love parameters of radial anisotropy. This gives rise to considerable tradeoffs which cannot be eliminated without further assumptions. Similar to the tradeoffs in the azimuthally averaged term, the 2ψ terms for Rayleigh waves depend simultaneously on 3 parameters. Only for Love waves are the azimuthal terms free of tradeoffs, depending on one elastic parameter each.

We selected overtones at 17 different frequencies for which we had more than 5,000 measurements each, with acceptable azimuthal coverage to be able to solve up to the 4ψ terms. The overtones have the periods of 153, 132, 114, 100, 88, 78, 70, 62, 56, 51, 47 and 43 seconds for the first overtone branch and 100, 89, 78, 69 and 63 seconds for the second overtone branch. Details of the measuring technique can be found in van Heijst and Woodhouse (1,2).

Construction of azimuthally anisotropic phase velocity maps

The azimuthally anisotropic phase velocity maps are constructed using a technique based upon the expansion in generalized spherical harmonics of the local phase velocity. Eq. (1) of the main text can be rewritten as $\frac{dc}{c}(\omega, \psi) = \alpha_0(\omega) + \tau_{ij}e_i e_j + \sigma_{ijkl}e_i e_j e_k e_l$ where e is a unit vector in the spherical surface in the direction of propagation of the surface wave ray. τ and σ are completely symmetric and trace free second and fourth rank tensors. The canonical contravariant components of these tensors (3) are related in a simple way to the 2ψ (τ^{++}, τ^{--}) and 4ψ ($\sigma^{++++}, \sigma^{----}$) terms in sine and cosine of propagation azimuth ψ . Path integrals of the phase velocity perturbation can easily be calculated in terms of the expansion coefficients of

τ^{++} and σ^{++++} by rotation to a coordinate frame in which the source-receiver path lies along the equator.

Searching for the strength of azimuthal anisotropy in the phase velocity maps

Constructing anisotropic phase velocity models amounts to adding more free parameters compared to the isotropic case. The important question is to know whether anisotropy explains the data better or whether a better variance reduction is merely due to an increased number of parameters. To investigate this, we add a weighting factor between isotropic and anisotropic terms in the cost function. The cost function is of the form $C = \epsilon + 1/\lambda|\nabla^2 m_0|^2 + \theta_2/\lambda|\nabla^2 m_2|^2 + \theta_4/\lambda|\nabla^2 m_4|^2$ where λ is an overall damping parameter which controls the tradeoff between data misfit ϵ and smoothness (Laplacian damping) of the 0ψ , 2ψ and 4ψ model components. θ_2 and θ_4 determine the relative strength of azimuthal anisotropy. Small values give preference to the isotropic terms and higher values allow more azimuthal anisotropy in the model. We minimize C many times varying systematically the different damping parameters. We plot the obtained misfit curves as unexplained data variance as a function of the number of used model parameters (trace of the resolution matrix) determined by λ . This gives us the overall strength of anisotropy required by the data for a given damping. The isotropic term is expanded to degree 40 and the anisotropic terms to degree 20 in generalized spherical harmonics which amounts to a total of 3405 free parameters. We typically invert for 500 independent parameters which gives a long wavelength model only. The over-parameterization together with the Laplacian damping avoids spectral leakage (4) in our models and gives an unbiased low degree expansion. We find that overall the data require the anisotropic terms ($\alpha_1(\omega) - \alpha_4(\omega)$) in Eq. (1) of the main text to be weighted 10 times less than $\alpha_0(\omega)$ (Fig. S3) giving thus preference to the azimuthally averaged term. Because the data decide upon the optimal strength of the azimuthal terms, the tradeoff between the different $\alpha_i(\omega)$ is small (Fig. S2).

Classical inverse theory versus Backus-Gilbert

Most often, in linear inverse problems, a cost function is defined which contains a term describing the fit to the data and a term allowing for constraints on the model parameters [e.g. R. Snieder and J. Trampert, *Inverse Problems in Geophysics*, (<http://samizdat.mines.edu>, 1999)]. In minimizing such a cost function, the compromise between fitting the data and constraining the model results in a model resolution showing generally strong oscillations which make a depth interpretation far from straight forward. In a Backus-Gilbert inversion the resolution kernel is optimized towards a desired shape which reduces the sidelobes considerably.

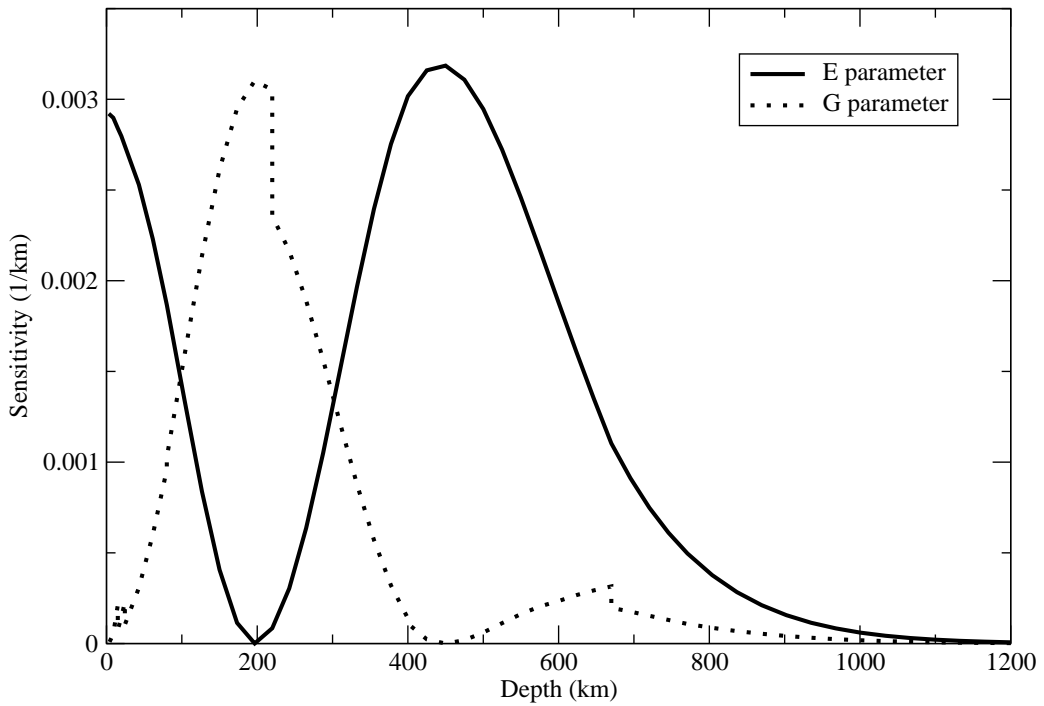


Fig. S1. Sensitivity kernels for the anisotropic parameters G and E calculated in PREM (5) for the first Love wave overtone at 132 seconds. The kernels specify how $\alpha_1(\omega)$ and $\alpha_2(\omega)$ (Eq. 1,

main text) are related to G and $\alpha_3(\omega)$ and $\alpha_4(\omega)$ are related to E as a function of depth. Note the strong sensitivity of the toroidal overtone to the 2ψ variation of the vertical shear velocity. A fundamental mode Love wave would have a G sensitivity about 10 times smaller.

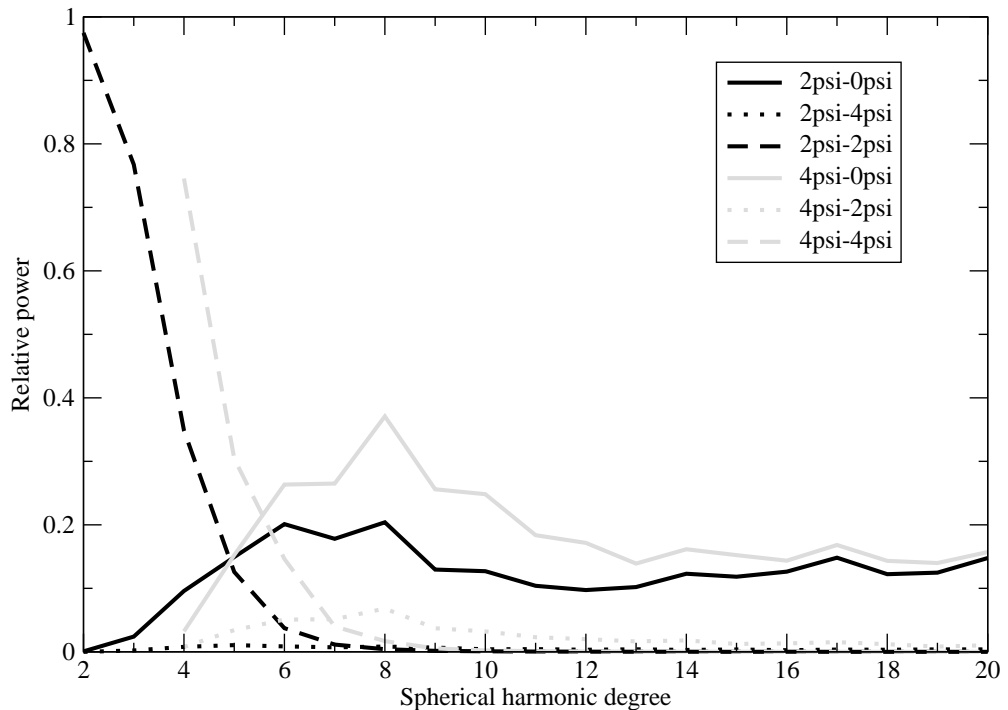


Fig. S2. Contracted resolution operator for the first Love wave overtone at 132 seconds. The full resolution matrix is a 3405 by 3405 matrix difficult to represent. Instead, we put a pure degree 0ψ , 2ψ or 4ψ input model through the resolution operator. We separate the output model in its 0ψ , 2ψ and 4ψ components and express their power relative to the total input power. This gives an indication of the resolution (diagonal block) and cross-talk between the different ψ components. The labels show the azimuthal components of the input and output model, respectively. An isotopic input model gave no contribution to azimuthal terms and the

corresponding curves are not shown here. The only existing tradeoff is from 2ψ and 4ψ terms to the isotropic ones which is of no consequence for this study. The implemented Laplacian damping shows as a rapid loss in resolution of the diagonal terms ($n\psi - n\psi$) with increasing degree. For different overtones, these diagonal terms have different slopes. Only degree 2 for 2ψ and degree 4 for 4ψ have the same resolution for all overtones.

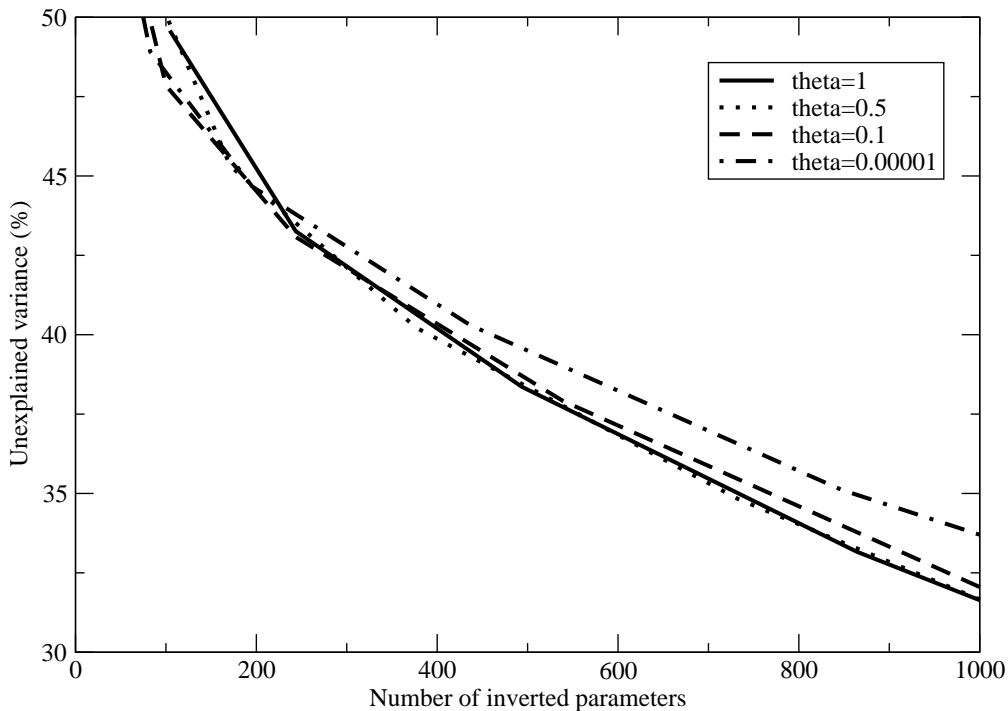


Fig. S3. Misfit curves for some selected values of relative anisotropic weights $\theta = \theta_2 = \theta_4$ as labeled on the figure. The smaller θ , the more weight is given to isotropic structures. Clearly, from 250 parameters onwards introducing anisotropy is more efficient in explaining the data. It is difficult to discriminate between the exact strength of anisotropy and a conservative point of view leads us to choose a weight of 0.1. The example shown is for the first Love wave overtone

at 132 seconds.

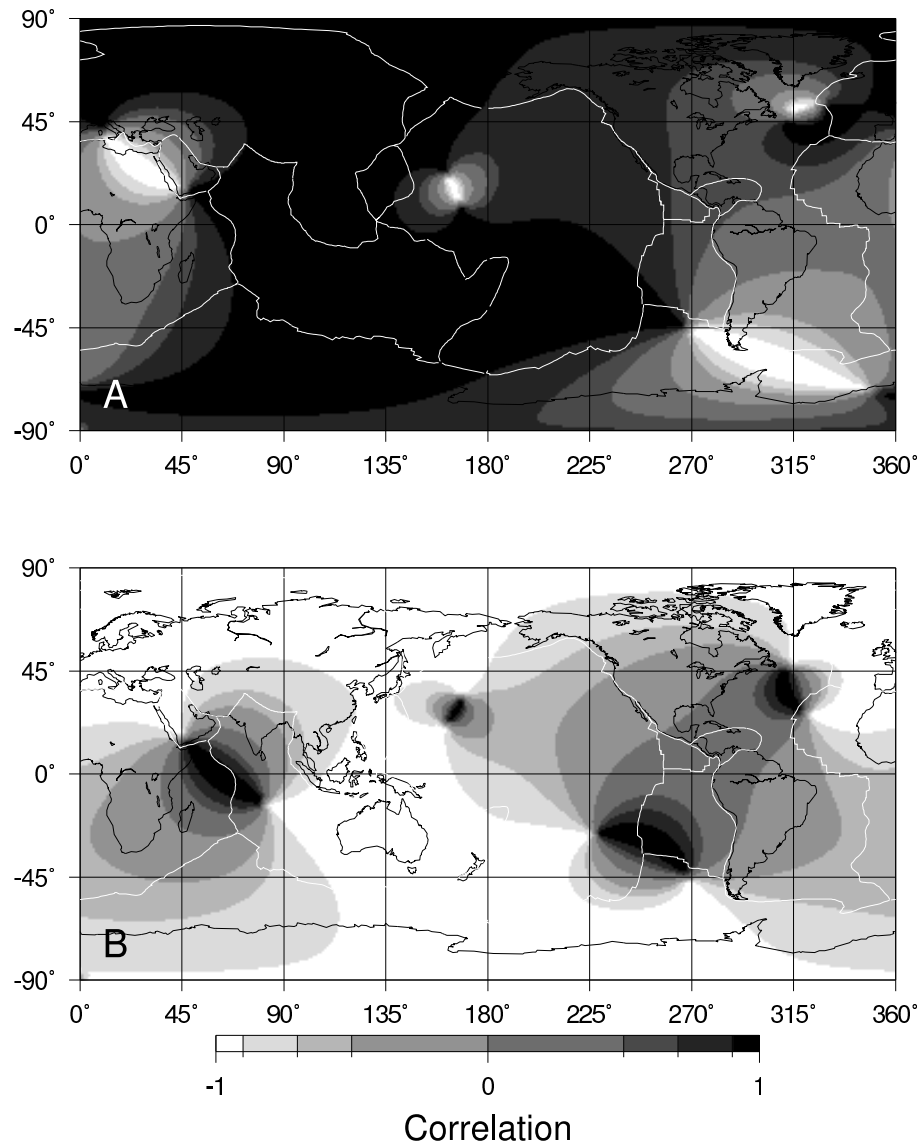


Fig. S4. Correlation between 2 fast directions Ψ_1 and Ψ_2 defined as $\cos(2 * (\Psi_1 - \Psi_2))$. If the 2 directions coincide, the correlation is 1, if they are perpendicular the correlation is -1. A: Correlation between the 2ψ term of the 100 second fundamental mode Rayleigh wave model and the corresponding Love wave overtone prediction (Fig. 2, main text). Poor correlation occurs where the amplitude of one of the fields is very low which makes it difficult to define

a direction. B: Correlation between the 2ψ term of the Love wave overtone prediction of the 100 second fundamental mode Rayleigh wave model (Fig. 2B, main text), which we take as a proxy (inverted from the same data set) to anisotropy in the shallower mantle, and our results for the transition zone (Fig. 3B, main text). In the Western Pacific and Eurasia the directions are perpendicular, but in other places, directions are closer.

References

1. H. J. van Heijst and J. H. Woodhouse, *Geophys. J. Int.*, **131**, 209, (1997).
2. H. J. van Heijst and J. H. Woodhouse, *Geophys J. Int.*, **137**, 601, (1999).
3. R. A. Phinney and R. Burridge, *Geophys. J. Royal astron. Soc.*, **34**, 451, (1973).
4. J. Trampert and R. Snieder, *Science*, **271**, 1257, (1996).
5. A. M. Dziewonski and D. L. Anderson, *Phys. Earth Planet. Int.*, **25**, 297, (1981).